

Influence of the Mounting Position and Sensor Orientation on Sensor Signals While Operated on a Multicopter Vehicle

Monika Scheibe¹, Klaus Dietl², Thomas Wiedemann³

¹ Deutsches Zentrum für Luft- und Raumfahrt (DLR), Institut für Physik der Atmosphäre, Oberpfaffenhofen, Germany

² Flugsensor, Andechs, Germany

³ Deutsches Zentrum für Luft- und Raumfahrt (DLR), Institut für Kommunikation und Navigation, Oberpfaffenhofen, Germany

Correspondence to: monika.scheibe@dlr.de

Abstract. We studied the influence of different sensor positions and different orientations on a multirotor (multicopter) platform. An optimal placement for the sensors should be found. Therefore several flight tests were performed using a DJI S900 multirotor with E1200 motor set. Therefore several gas sensors and small optical particle counters (OPC) were attached to the copter. The gas sensors are alphasense's four electrode electrochemical cells for sulfuric acid (SO₂) and carbon monoxide (CO). The OPC is an alphasense optical particle sensor version N2. The OPC flights were performed and compared to measurements undertaken on a mast. It became apparent that not any position of a sensor on a multicopter promises an authentic atmospheric dataset. When using the particle sensors the position influence was overwhelming.

1. Theory of operation and characterization of alphasense mini-OPC

Alphasense OPC version N2 operates a laser LED at typically 5-8 mW (max. 25 mW) at a wavelength of 658 nm. The measuring principle is light scattering by individual particles. The light path encounters a cone under an angle of 22° is being scattered by particles, impacts a mirror and is directed to detector. Different groups already characterized and evaluated the sensor during ground based measurements (Crilley, et al., 2018) (Sousan, et al., 2016). To our knowledge a copter based airborne characterization was not published so far.

2. Influence on Sensor Position Regarding a Small OPC

Several tests were performed with two Alphasense Optical Particle Counters (OPC) installed on the flying copter platform and for comparison on a mast.

For studies about the difference between mounting positions on the copter platform field measurements FM01 and FM02 were performed. For studies about the OPC virtual impactor behavior influence FM03 was performed.

2.1 Observations during FM01 / FM02

One OPC sensor was mounted on the top side while the second was installed below the platform. To eliminate sensor individual effects the same test was performed twice with alternating positions of both sensors. The copter performed a self-regulated hover flight approximately 15 m above the same spot for 10 minutes each flight with wind flow coming mostly from the ahead direction. The inlets were both looking towards the center of the copter frame, thus meaning the OPCs were installed upright as the manufacturer recommends an installation of the inlet

opening perpendicular to the main direction of (wind induced) airflow to mitigate the effects of wind direction on sampling (Alphasense Ltd, 2015). This secures vertical flow induced by propulsion and normal flow induced by wind velocity across the sensor opening. Sampling time was about 1.4 Hz counting rate. Before the flights both sensors were mounted for 45 minutes on a tower 15 m above the ground. For the comparison in the following histogram only the later 20 min are included. After the flights both sensors were mounted again for 15 minutes at the same place on the tower to be sure that number concentrations did not change much during the flights. To compare to all other measurements, 10 minutes of number concentrations were doubled to interpolate to 20 minutes of measurement time.

OPC data and instrumental parameters are stored locally to onboard SD card in ASCII format when operated in standalone mode (no PC connection). Data analysis converts counting rates to particle number concentrations per size bin by division by the volumetric flow rate. Number concentrations (n_{meas}) were corrected for standard pressure and temperature conditions (n_{corr}) according to the ideal gas law by using pressure and temperature data measured on board the copter (suffix “h”) and standard pressure and temperature conditions (suffix “0”):

$$n_{corr} = n_{meas} * \frac{p_0 * T_h}{p_h * T_0} \quad (1)$$

$$p_0 = 1013.15 \text{ hPa}$$

$$T_0 = 273.15 \text{ K}$$

The results of this test are three histograms overlaid in one graph. One histogram represents the statistical sum of sampled data for both sensors in case of the top side position during hover (20 min in total; yellow line), the other histogram shows the statistical sum when the sensors were mounted below the copter platform during hover (20 min in total; blue line). The third one shows data from the static measurement on the tower (20 min in total; solid black bars). Note: The following histograms have to be understood as qualitative size information only and do not represent proper particle number size distributions.

Figure 1 and Figure 2 show results from different sensor positions. In Figure 1 each the upper and the lower sensor were positioned on the edge of the center frame with inlets orientated normal to the propulsion air flow. In Figure 2 each the upper and the lower sensor were positioned almost in the middle of the center frame with inlets orientated normal to the propulsion air flow.

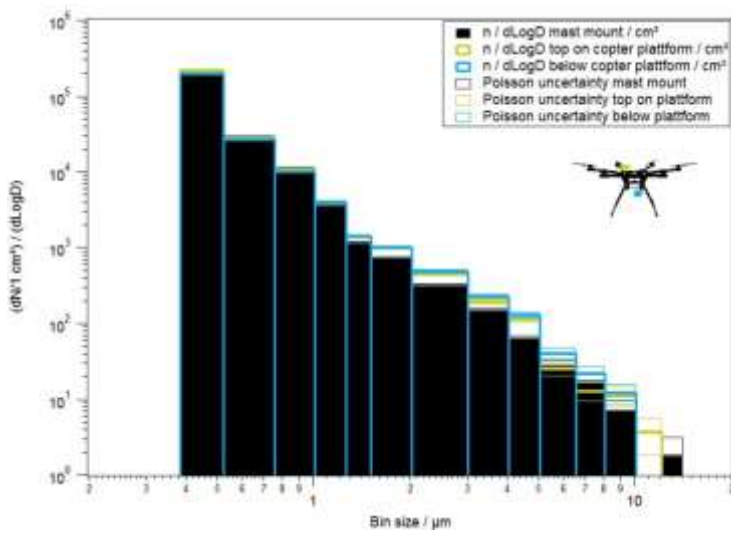
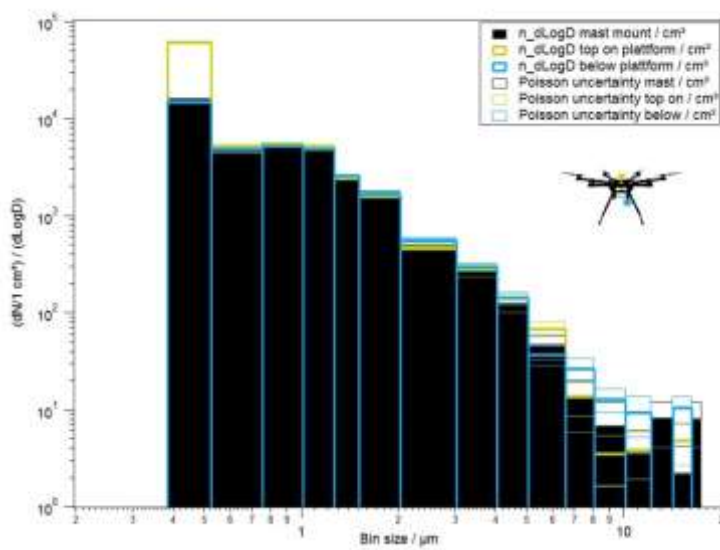


Figure 1 Particle size distribution histogram of spherical equivalent size (based on RI of 1.5) Comparison of different OPC mounting positions; measurements on August, 10th, 2017 (FM01)



5 Figure 2 Particle size distribution histogram of spherical equivalent size (based on RI of 1.5). OPC mounting position with inlet looking aside; measurements on August, 21st 2017 (FM02)

The first striking detail is that all particle measurements performed on the (flying) copter platform fit well between sizes from 0.52 μm (Bin01) to 1.25 μm (Bin03) (during FM01) respectively to 3 μm (Bin06) (during FM02) only.

10 Although the count-statistical error is high for small count rates, in most cases larger particles tend to be overestimated, especially, when the sensor is mounted below the frame. The biggest particles (larger than 10 μm ; Bin12 to Bin15) are not or badly seen.

According to the manufacturer the OPC has dynamic correction for sample flow-rate. This is realized by changes of the fan speed (Alphasense Ltd, 2015). The mean sample flow rate (SFR) while mounted on the mast was 3.15 ml/s. During the bottom-side measurements of the platform it increased about 4.1 % (3.28 ml/s) while the mean flow rate on top decreased about 9.3 % (2.86 ml/s). Variations like wind direction in the vicinity of the OPC are monitored and corrected dynamically by the OPC so that the particle concentrations are unaffected by moderate flow variations (Alphasense Ltd, 2015).

The bottom-side measurements (blue lines) overestimate particles between 1.25 μm to 16 μm more than top-side (yellow lines) mounted sensors. From dynamic flow studies, e.g. (Eu, et al., 2014) or (Sandstrom, 2017), this observation can be explained with over counting due to a vortex field which traps heavier particles. The deviation between copter based samples and mast data may also be explained by different air volumes that contribute to the different samples: Air probing on the mast only “sees” the sensor surrounding air while the sensor on the copter “sees” a larger air volume caused by the propeller intake (see other publication).

Comparing Figure 1 and Figure 2 the best position for a particle sensor seems to be at the frames’ edge and on the top of the frame with an inlet orientation normal to the air flow.

2.2 Observations FM03

To learn about scattering behavior and the effects by platform induced flows two sensors were mounted with upward pointing inlet pointing into the flow at two different positions on the copter platform. Keep in mind that this orientation is not the manufacturer recommended sensor heading in the ambient air flow. To eliminate influence of the individual OPC a second flight was performed with alternating positions of the two OPC. In the final data set number concentrations of both sensors at one position are summed.

The challenge now is that we compare size distributions of different flow regimes. If mast mounted data shall be regarded as comparable to data sampled in the air stream we have to regard the order of calculated flow rate of the sensor as realistic: Due to sensor design mass flow rate through the sensor is estimated by current a fan (instead of a pump) needs to run. If we assume that by the propellers air is pressed through the inlet the flow rate might be miscalculated. On the other hand side the fan occurs also as a resistance to the propeller induced flow by the copter so that the calculated flow rate can be assumed as real for the following interpretation.

From impactor theory in this configuration large particles are expected to accumulate while small particles are expected to be depleted based on flow paths the smaller particles can follow easier.

In Figure 4 the upper sensor was positioned at the edge of the center frame and the lower sensor was positioned at the landing gear, both with inlets orientated upwards into the propulsion air flow and air stream through the sensor is parallel to the surrounding airflow. We observe that for the on top mounted sensor the qualitative size distribution is comparable to the top mounted horizontal oriented inlet.

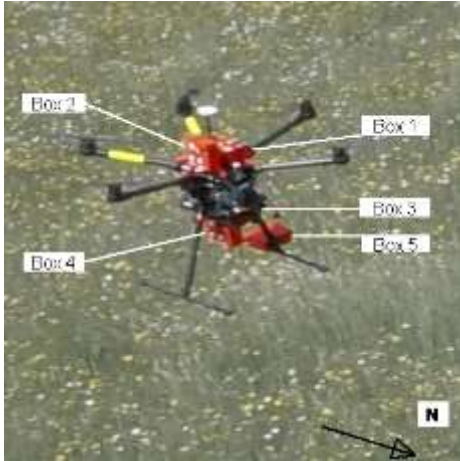
3.1 Position and Orientation Effects on a Gas Sensor Signal

In total five boxes with calibrated electrochemical gas sensors for sulfuric acid (SO_2) and sensors for carbon monoxide (CO) were mounted at once on a DJI E1200 platform to study the influence of sensor positioning and sensor orientation on the sensor signal.

Two of the sensor boxes were mounted on top of the platform: one box with skywards looking sensors (as a downward orientation towards the frame would make no sense) and one box with sideward sensor orientation. Two further boxes were mounted below the platform: one box with downward looking sensors and one box with sideward sensor orientation – the same side as the above mounted sensor. A sensor mounted far below the platform would be mounted preferably looking downwards to prevent heating of the sensor by solar radiation and direct sun light as well as to protect it from falling objects like rain. That’s why the fifth sensor box was mounted on the landing gear looking downward. During flight, the platform’s heading always was the same with yellow marked

arms showing south. Flights were performed around noon. Sensors of boxes no. 1, 2 and 4 were exposed directly to the sun while sensor box no. 3 was completely shadowed by the platform and sensors of box no. 5 were shadowed by the box itself (Figure 4).

To gain a better sensor signal a small fire was lit fed with wood and charcoal (material: $\sim 10 \text{ cm}^3$) in an alloy trough placed in a slightly sloping meadow. Thermals and slow turbulence carried the smoke in alternating directions away from the fire spot. The copter was flown several times around the fire spot at different altitudes and crossed the smoke plume several times (Figure 3 Sensor mounting positions Figure 4 Sensor flight path).



10 **Figure 3 Sensor mounting positions**

Figure 4 Sensor flight path with constant copter heading

Background concentration is taken from a nearby Global Atmosphere Watch (GAW) station operated by German Weather Service (DWD). The observatory is located at 47.8011°N 11.0246°E and is therefore around 30 km away as the crow flies at 934 m ASL and thus a good 200 m higher than the measuring meadow of the experiment (713 m ASL). As there is no closer measuring station available for qualified gas measurements, we use these data to obtain an orientation of the background level of the gas concentrations. Certainly, they cannot be used as absolute values for comparison. The concentrations occurring locally on the measuring site may also be influenced by surrounding connecting roads and the local mean concentration may differ from the concentrations occurring at the observatory. The mean value for the flight period between 11-14 h on May 19th was found to be 137.9 ppb for CO and $0.147 \text{ ppb} \pm 0.025 \text{ ppb}$ for SO₂. This data was kindly provided by the German Weather Service (DWD).

20 **4. Results for gas sensor mounting and orientation**

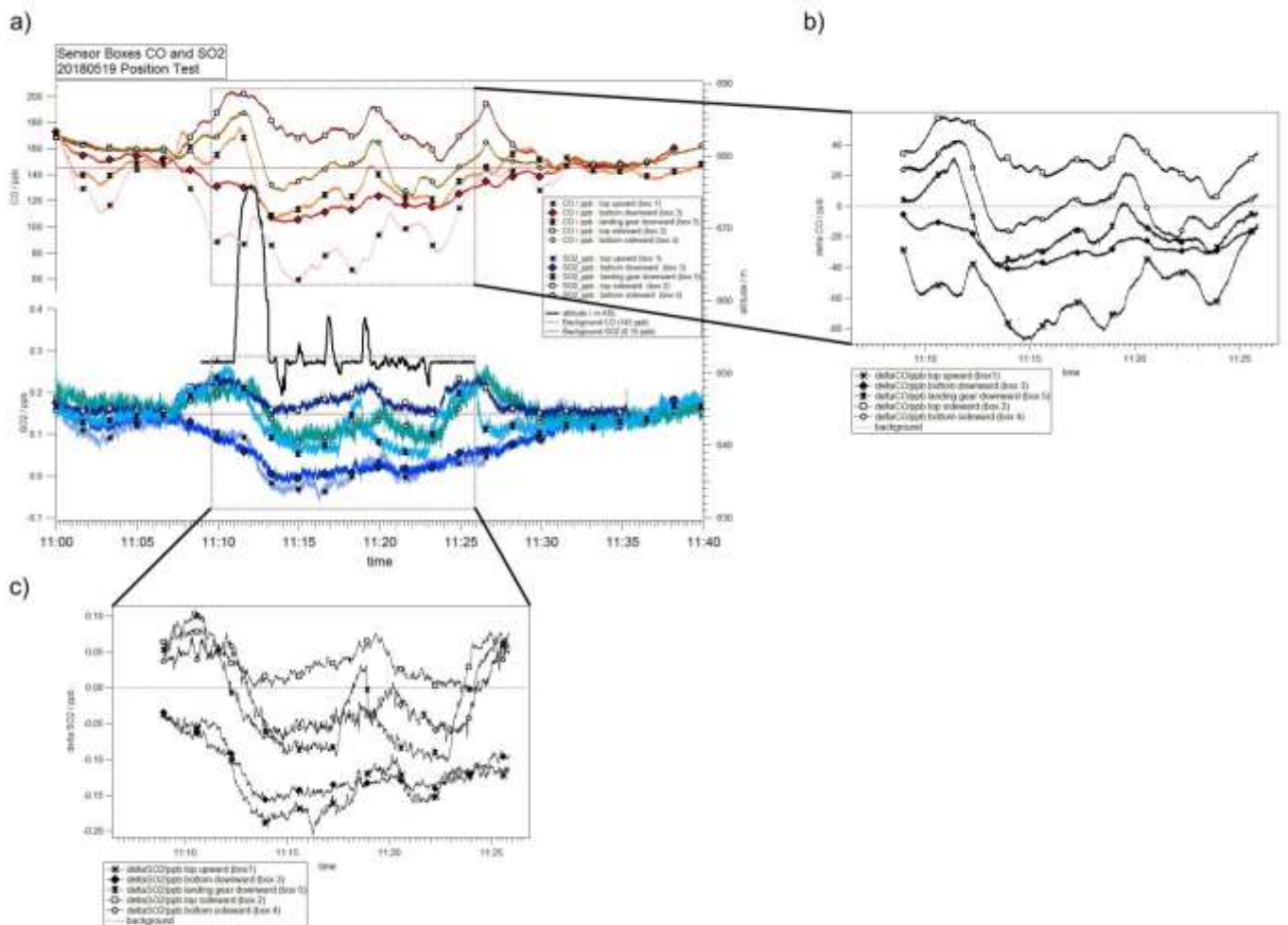
Although both gas measurements mostly lead to the same conclusions we regard CO measurement (Figure 3a and b) as the guiding signal through our observations as SO₂ concentration was diluted almost down to the detection limit of the sensors (Figure 3a and c).

First of all, being directly exposed to the sun obviously has no big impact on the gas measurement. The most striking of the flight signal sequence is the upward showing sensor on top of the platform (x-ed marked line). Straight encounter to the propeller's airflow not only seem to distort the measurement but also leads to the strongest underestimation of the CO and SO₂ gas concentration and a signal delay in parts. The downward facing sensors (solid symbols) underestimate the concentration compared to the sideward facing sensors (white symbols). The landing gear mounted sensor detects the highest concentration before flight when the copter was standing in the

meadow on the ground. This may be argued with CO emitted by bacteria in the soil (Sobieraj, et al., 2022) or by cross sensitivities of the electrochemical cell. With respect to sensor reaction time ($t_{90} < 25$ s for CO; $t_{90} < 40$ s for SO₂) the signal falls far below CO background concentration with takeoff.

The top mounted sensor facing sideward shows the most vivid structured CO signal and also the highest concentrations.

The downward looking sensor mounted below the platform obviously shows the most smoothing and time lagged signal structure. It also shows a low concentration.



10 **Figure 3 CO and SO₂ measurement before, during and after the flight with zoomed delta CO during the flight. The mean value taken from all sensors is represented by the thin straight line.**

5. Results for Optical Particle Sensor mounting and orientation

For the alphasense OPC we observe a confirmation of the expectation from impactor theory: There are some few counts of large particles in the copter based data while there are almost none in the mast data found. The sensor position above the frame seems to be more representative compared to the mast measurement than the below the frame mounted position. A look back to [companion paper “Technical Note_20180605_Using Unmanned Multicopter Vehicles for Atmospheric Research and Air Quality Measurement”; Figure 7] might help to explain that: The upper sensor is positioned in a much more quiet and steady flow environment than the bottom mounted sensor where air is pressed into the rotor flow tubes and which have to be assumed to be turbulent.

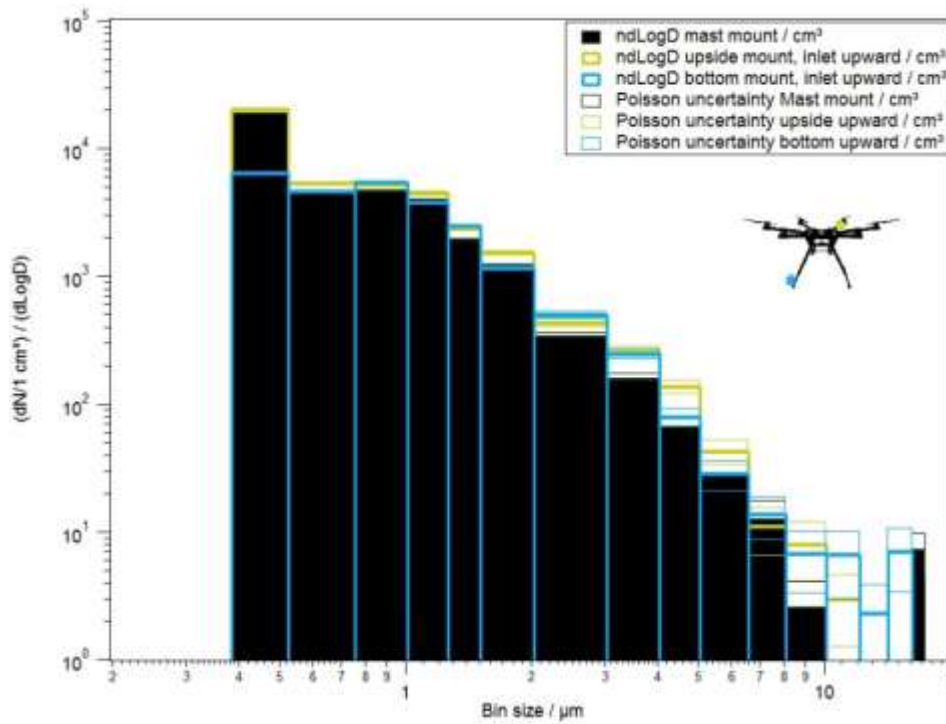


Figure 4 Particle size distribution histogram of spherical equivalent size (based on RI of 1.5). OPC mounting position with upward looking inlet; measurements on August, 21st 2017 (FM03)

5 As already shown in part 2.1 Observations during FM01 / FM02, suction height and air intake volume during copter based measurements probably deviates from suction height during mast measurements. The propulsion system sucks air from above the rotors below the platform to compensate gravity. This might result in different particle size distributions due to different air masses. Further studies on impactor collection efficiency with repeated numerical analysis are necessary to determine the exact streamline pattern and particle trajectories for a given size
10 of the Alphasense OPC geometry.

To understand the different behavior of OPC position and inlet orientation we also performed studies with a TSI 3475 Condensation Monodisperse Aerosol Generator which is able to produce high number concentrations. We tested a direct inflow into the OPC (inlet parallel to the air stream), and also an orientation of the inlet normal to the surrounding air flow. Different surrounding flow velocities were simulated by a fan in a wind tunnel. Particles
15 with a defined small size distribution are produced while using DEHS (Di-2-ethyl-hexyl-sebacate; formula: C₂₅H₅₀O₄) and a sodium solution (20 mg/l NaCl). The principle of the TSI 3475 is based on controlled heterogeneous condensation.

Table 1 shows the refractive index and the corresponding wave length of DEHS:

Table 1 Characteristics of DEHS

Refractive index	Wave length (nm)
1.4500	650
1.4520	600
1.4535	550
1.4545	500
1.4585	450

Table 2 shows that in order to change produced particle size by the TSI 3475 only the saturator temperature was changed; leaving all other parameters like flows static:

5 **Table 2 Parameters of TSI 3475**

Particle size	Saturator Flow / (l/h)	Screen Flow / (l/h)	Saturator Temperature / °C	Reheater Temperature / °C	Total Flow / (l/h)
Small	28	135	170	300	225
Medium	28	135	215	300	225
Large	28	135	245	300	225

A direct inflow into the OPC (inlet parallel to the air stream), forced by a fan in a wind tunnel, shifts particle distributions towards smaller sizes and slightly larger count numbers independent on the aimed particle size (see Figure 5 for small particles, Figure 6 for medium particles, Figure 7 for large particles).

10

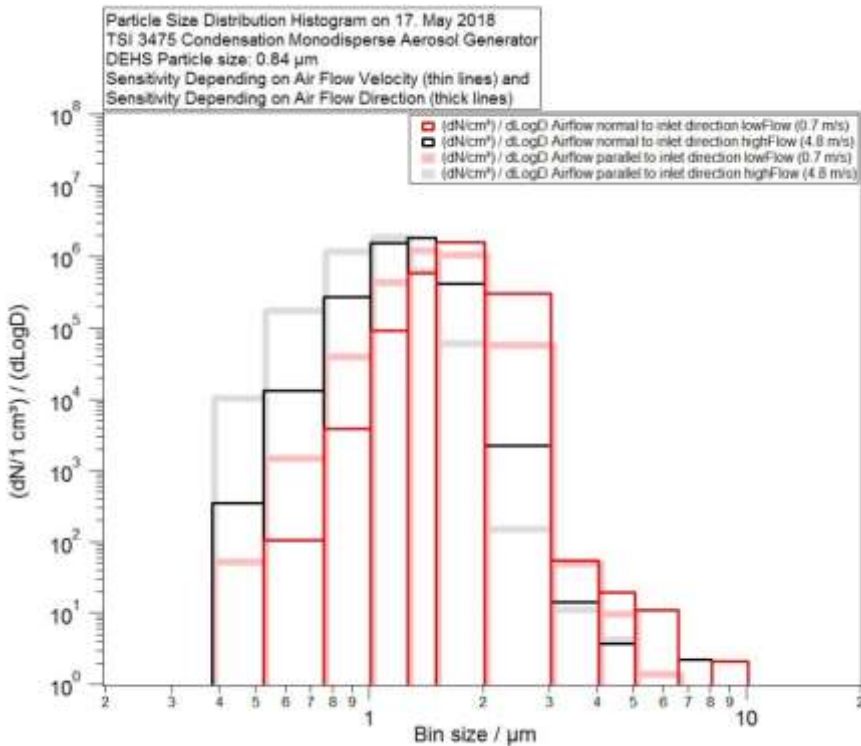


Figure 5 Forced inflow into the OPC shifts small test particle size distribution towards smaller sizes and larger count numbers particles (red -> black); turning the sensor from inlet pointing normal to surrounding air flow to pointing parallel into the surrounding air flow also leads to a shift towards a smaller size distribution as well as slightly raised count rates (red -> rosé; black -> grey)

15

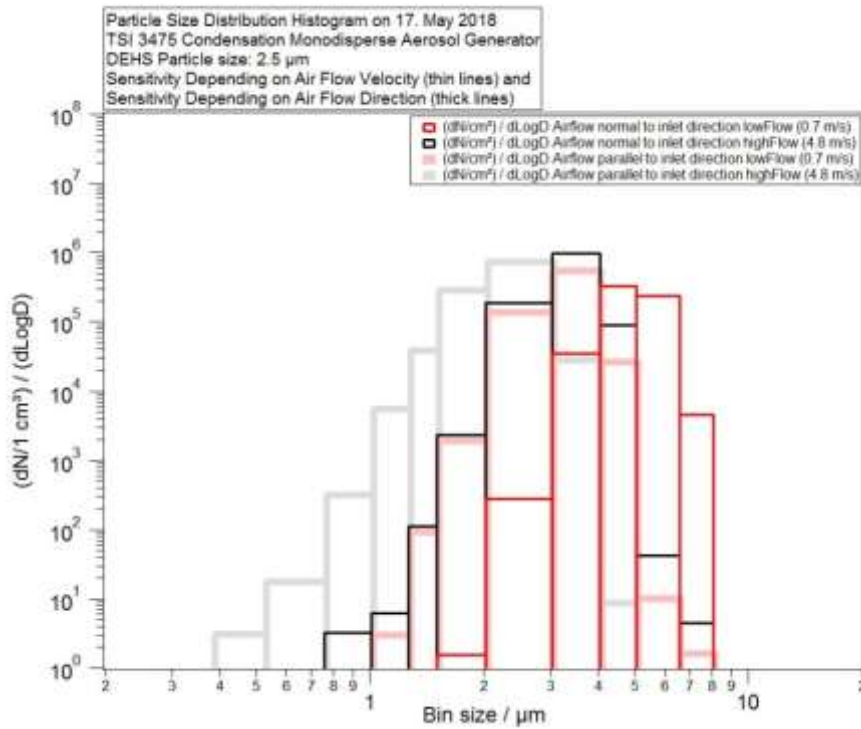


Figure 6 Forced inflow into the OPC shifts medium test particle size distribution towards smaller sizes and larger count numbers particles (red -> black); turning the sensor from inlet pointing normal to surrounding air flow to pointing parallel into the surrounding air flow also leads to a shift towards a smaller size distribution as well as slightly raised count rates (red -> rosé; black -> grey)

5

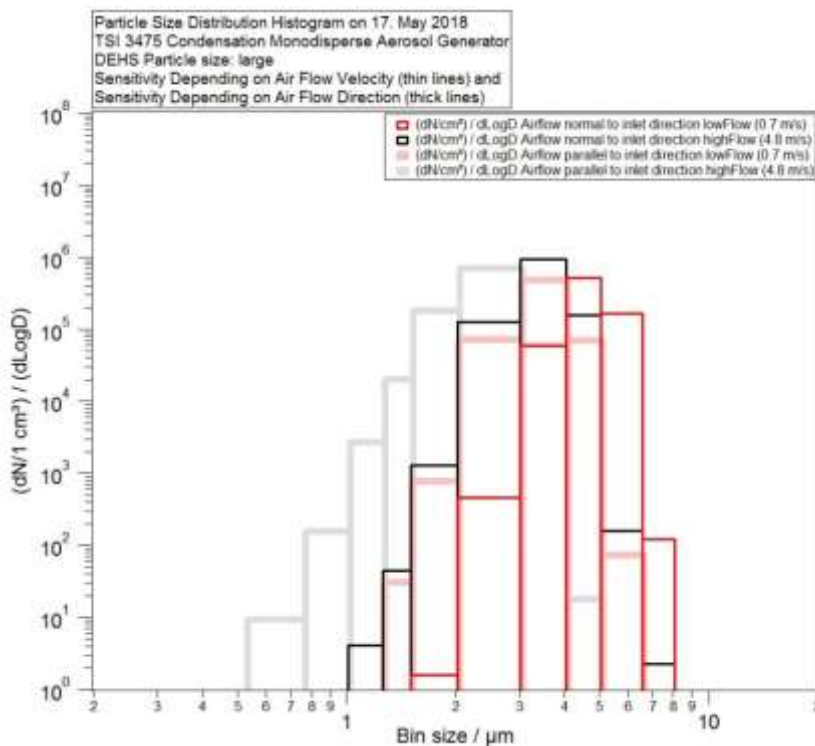


Figure 7 Forced inflow into the OPC shifts large test particle size distribution towards smaller sizes and larger count numbers particles (red -> black); turning the sensor from inlet pointing normal to surrounding air flow to pointing parallel into the surrounding air flow also leads to a shift towards a smaller size distribution as well as slightly raised count rates (red -> rosé; black -> grey)

10

This results in a sensor position for the alphasense OPC with an inlet orientation normal to the propeller induced flow of the surrounding air. To avoid large velocities the sensor should be mounted on the top side of the center frame best far away from fast air flows– better even slightly elevated.

References

- Alphasense Ltd. 2015.** *Alphasense User Manual OPC-N2 Optical Particle Counter 072-0300*. [PDF Document]. Essex.CM77 7AA. UK : s.n., December 2015. Issue 5.
- 5 **Crilley, Leigh R., et al. 2018.** Evaluation of a low-cost optical particle counter (Alphasense OPC-N2) for ambient air monitoring. *Atmospheric Measurement Techniques*. 2018, Vol. 11, pp. 709–720.
- Eu, Kok Seng and et al. 2014.** An Airflow Analysis Study of Quadrotor Based Flying Sniffer Robot. *Applied Mechanics and Materials*. 04 07 2014, Vol. 627, pp. 246-250.
- Sandstrom, Tim. 2017.** Exploring Drone Aerodynamics with Computers. *National Aeronautics and Space Administration*. [Online] NASA, 11 January 2017. [Cited: 28 June 2017.] <https://www.nasa.gov/image-feature/ames/exploring-drone-aerodynamics-with-computers>.
- 10 **Sobieraj, Karolina, et al. 2022.** Carbon Monoxide Fate in the Environment as an Inspiration For Biorefinery Industry: A Review. *Frontiers in Environmental Science*. 02 2022, Vol. 10.
- Sousan, Sinan, et al. 2016.** Evaluation of the Alphasense Optical Particle Counter (OPC-N2) and the Grimm
- 15 Portable Aerosol Spectrometer (PAS-1.108). *Aerosol Science and Technology*. 2016, Vol. 50(12), pp. 1352–1365.